Kobe University Repository : Kernel

PDF issue: 2025-05-25

CRITICAL DIAMETER FOR LIFT REVERSAL OF BUBBLES IN LINEAR SHEAR FLOWS

Hayashi, Kosuke

Lucas, Dirk

Legendre, D.

Tomiyama, Akio

(Citation)
Multiphase Science and Technology,33(2):69-85

(Issue Date)
2021

(Resource Type)
journal article

(Version)
Accepted Manuscript

(Rights)
© 2021 by Begell House, Inc. www.begellhouse.com

(URL)
https://hdl.handle.net/20.500.14094/90009448

CRITICAL DIAMETER FOR LIFT REVERSAL OF BUBBLES IN LINEAR SHEAR FLOWS

K. Hayashi,[1,] D. Lucas,[2] D. Legendre,[3] & A. Tomiyama[1]*

[1]*Graduate School of Engineering, Kobe University, 1-1 Rokkodai, Nada, Kobe, 657-8501, Japan*

[2]*Helmholtz-Zentrum Dresden-Rossendorf, Institute of Fluid Dynamics, Bautzner Landstraße 400, 01328 Dresden, Germany*

[3]*Institut de Mécanique des Fluides de Toulouse (IMFT) - Université de Toulouse, CNRS-INPT-UPS, 2 Allée du Professeur Camille Soula, 31400 Toulouse, France*

*Address all correspondence to: K. Hayashi, Graduate School of Engineering, Kobe University, 1-1 Rokkodai, Nada, Kobe, 657-8501, Japan,
E-mail: hayashi@mech.kobe-u.ac.jp

Original Manuscript Submitted: mm/dd/yyyy; Final Draft Received: mm/dd/yyyy

The lift coefficient C_L of a bubble in a shear flow is known to change its sign depending on the bubble shape, i.e. C_L of spherical bubbles are positive for any bubble Reynolds numbers while those of ellipsoidal bubbles can be negative due to the deformation-induced negative lift. The critical bubble diameter, d_C, for the lift reversal was discussed in this study by making use of available C_L correlations for clean bubbles in linear shear flows. As a result, the following conclusions were obtained: (1) the C_L correlations well describe the complex characteristics of d_C and the lift reversal criterion in terms of Re_C is well reproduced with the correlations, (2) in the surface tension and inertial force dominant regime, the critical Eötvös and Weber numbers can be used to develop a simple criterion of lift reversal, i.e. they are almost constant, and the capillary number for d_C can be expressed in terms of the Morton number only, M; these dimensionless groups in the viscous force dominant regime however show more complex dependence on M, and (3) the critical Ohnesorge number, Oh_C, monotonically increases with increasing M even in the viscous force dominant regime. Therefore a tentative d_C correlation based on Oh_C was developed.

KEY WORDS: *lift force, lift reversal, negative lift, shape deformation*

1. INTRODUCTION

Knowledge on the lift force acting on a bubble moving in liquid is of great importance to predict distributions of the gas volume fraction (void fraction) in bubbly flows. There have therefore been many studies on the lift force by means of theoretical analyses, experiments and numerical simulations (Adoua et al., 2009; Aoyama et al., 2017; Auton, 1987; Auton et al., 1988; Bothe et al., 2006; Dijkhuizen et al., 2010; Ervin and Tryggvason, 1997; Hessenkemper et al., 2020; Lee and Lee, 2020; Legendre and Magnaudet, 1997, 1998; Li et al., 2016; Tomiyama, 1998; Tomiyama et al., 2002b; Žun, 1980; Ziegenhein et al., 2018). The lift coefficient, C_L, of a deformed bubble in a linear shear flow is known to be either positive or negative, and the critical bubble diameter, d_C, for the change in the sign, i.e. the lift reversal, has often been discussed so far because of its practical importance in engineering, e.g. the transition from a wall-peak to a

 © 2021 by Begell House, Inc. www.begellhouse.com

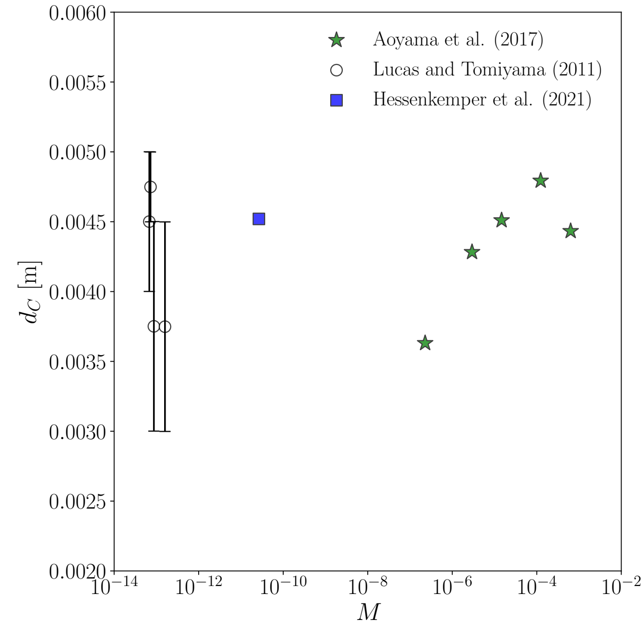

FIG. 1: Critical bubble diameter, d_C (Aoyama et al., 2017; Hessenkemper et al., 2021; Lucas and Tomiyama, 2011).

core-peak void fraction profile in a bubbly pipe flow can be described by the change of the sign of C_L and the lift has a potential to make the flow structure of a bubbly flow in a bubble column unstable if the sign is negative (Lucas et al., 2005; Lucas and Tomiyama, 2011).

Figure 1 shows critical bubble diameters reported in literature. The circle and square symbols are data of low Morton number systems (Hessenkemper et al., 2021; Lucas and Tomiyama, 2011). Hessenkemper's data were for single air bubbles in linear shear flows of purified water, whereas d_C of Lucas' data were determined from void fraction distributions of steam-water bubbly pipe flows; the void fraction profile of each bubble size class was measured and d_C was determined as the diameter at which a transition from a wall-peak to a core-peak profile took place. The data of Aoyama et al. (2017) were obtained for air bubbles in linear shear flows of glycerol water solutions. Interestingly, in spite of the wide range of the Morton number M, d_C does not change so much and ranges from about 3 to 5 mm. Here M is defined by

$$M = \frac{\mu_L^4 \Delta\rho g}{\rho_L^2 \sigma^3} \tag{1}$$

where μ_L is the liquid viscosity, $\Delta\rho$ the density difference between the two phases, g the acceleration of gravity, and σ the surface tension. The dependence of d_C on M is however complicated.

The critical diameters are re-plotted in terms of the critical bubble Reynolds number, Re_C, and M in Fig. 2, where the bubble Reynolds number is defined by

$$Re = \frac{\rho_L V_R d}{\mu_L} \tag{2}$$

where d is the sphere-volume-equivalent bubble diameter, and V_R the bubble velocity relative to

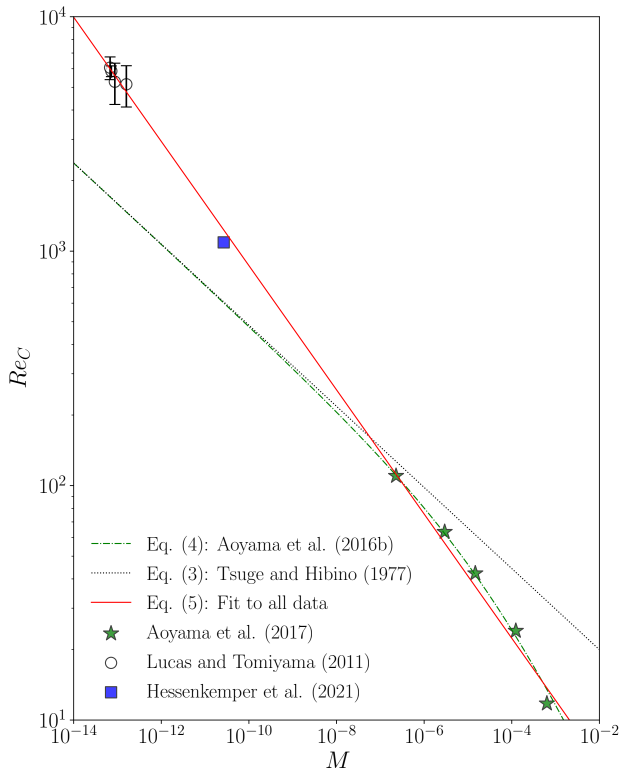

FIG. 2: Critical bubble Reynolds number, Re_C. Eq. (18) is used to evaluate Re_C from the d_C data of Lucas and Tomiyama (2011).

a liquid velocity. The dotted line represents the critical bubble Reynolds number, Re_O, for the onset of path oscillation of bubbles in a stagnant liquid (Tsuge and Hibino, 1977):

$$Re_O = 9.0M^{-0.173} \tag{3}$$

Aoyama et al. (2017) pointed out that Re_C shows a dependence similar to Re_O and utilized Re_O to correlate their Re_C data as follows: (Aoyama et al., 2016b)

$$Re_C = \frac{Re_O}{(1 + 14M^{0.29})^{0.89}} \tag{4}$$

This equation was developed so as to approach Re_O at low M. However actual Re_C are much larger than Re_O in the low viscosity systems. All the data can be roughly fitted by the following equation as shown by the solid line:

$$Re_C = 2.01M^{-0.264} \tag{5}$$

Though this equation gives reasonable evaluations of Re_C, we have not sufficiently understood a physical ground of this curve and the complex behavior of d_C.

In this study we investigate the characteristics of d_C and Re_C by making use of lift coefficient correlations for clean bubbles recently proposed in Hayashi et al. (2021, 2020) to further understand the lift reversal criteria.

2. LIFT CORRELATIONS

Correlations utilized to investigate d_C are summarized in the following. The shear-induced lift force acting on a bubble is expressed by (Žun, 1980)

$$\boldsymbol{F}_L = -C_L \left(\frac{\rho_L \pi d^3}{6} \right) \boldsymbol{V}_R \times \nabla \times \boldsymbol{V}_L \tag{6}$$

where $\boldsymbol{V}_R$ is the bubble relative velocity, and $\boldsymbol{V}_L$ the liquid velocity. We proposed the following empirical correlation to express C_L with lift reversal in the viscous force dominant regime (the μ regime) (Hayashi et al., 2020):

$$C_L = C_L^S - \frac{g(M)(\chi - 1)^{h(M)}}{Re} \tag{7}$$

where χ $(= d_H/d_V)$ is the aspect ratio of a bubble, d_H and d_V are the major and minor axes of the ellipsoidal bubble and the functions, g and h, are

$$g(M) = a \exp(-bM^c); \quad h(M) = p \exp(-qM^r) \tag{8}$$

The constants are given by $a = 500$, $b = 6.0$, $c = 0.0735$, $p = 3.46$, $q = 5.4$ and $r = 0.191$, which were determined by making use of Aoyama's lift data for $-6.6 \leq \log M \leq -3.2$. The C_L^S is the lift coefficient of a spherical bubble proposed by Legendre and Magnaudet (1998):

$$C_L^S = ([C_L^{SL}]^2 + [C_L^{SH}]^2)^{1/2} \tag{9}$$

where the lift coefficients of a low Reynolds number bubble, C_L^{SL}, and a high Reynolds number bubble, C_L^{SH}, are given by

$$C_L^{SL} = \frac{6}{\pi^2} \frac{2.255}{\sqrt{SrRe}\,[1 + 0.2Re/Sr]^{3/2}} \tag{10}$$

$$C_L^{SH} = \frac{1}{2} \left(\frac{1 + 16/Re}{1 + 29/Re} \right) \tag{11}$$

Here the dimensionless shear rate, Sr, is defined by

$$Sr = \frac{\Omega d}{V_R} \tag{12}$$

where Ω is the vorticity of a linear shear flow. Equation (7) assumes that the upperbound of the lift coefficient is C_L^S (the first term). The second term expresses the negative lift component constructed based on the following physical arguments: the negative lift is induced by the vorticity, ω, produced at the bubble surface (Adoua et al., 2009), which increases with increasing χ, the drag is proportional to the vorticity (Legendre, 2007), and the viscous contribution appears in the lift of a spherical bubble in the form of Re^{-1} (Legendre and Magnaudet, 1998).

A C_L correlation for the surface tension-inertial force dominant regime (the σ-i regime) was also proposed by accounting for the relation between the drag and the lift (Hayashi et al., 2021):

$$C_L = C_L^S - \gamma_e \omega_{\max}^{*\infty}(\chi) \left[\frac{8}{3} \frac{Eo}{Eo + 16(\chi^2 - 1)/\chi^{8/3}} \right] \tag{13}$$

where $\gamma_e = 0.048$ and $\omega^{*\infty}_{\max}$ is the dimensionless maximum vorticity in the infinite Reynolds number limit (Magnaudet and Mougin, 2007)

$$\omega^{*\infty}_{\max}(\chi) = \frac{2\chi^{5/3}(\chi^2 - 1)^{3/2}}{\chi^2 \sec^{-1}\chi - (\chi^2 - 1)^{1/2}} \tag{14}$$

Equation (13) was validated for Hessenkemper's air-water data, whose M is 2.63×10^{-11} ($\log M = -10.58$).

In the μ regime, the drag coefficient, C_D, can be evaluated by using the following empirical correlation (Chen et al., 2019):

$$C_D = \frac{16}{Re}\left(1 + 0.25\chi^{1.9}Re^{0.32}\right) \tag{15}$$

The following shape correlation gives good evaluations of χ for a wide range of M, i.e. $-11 \leq M \leq 0.63$ (Aoyama et al., 2016a):

$$\chi = (1 + 0.016Eo^{1.12}Re)^{0.388} \tag{16}$$

where Eo is the Eötvös number defined by

$$Eo = \frac{\Delta\rho g d^2}{\sigma} \tag{17}$$

In the σ-i regime, Tomiyama et al. (1998) proposed the following correlation based on a wave analogy (Mendelson, 1967):

$$C_D = \frac{8}{3}\frac{Eo}{Eo + 4} \tag{18}$$

The shapes of bubbles rising through purified water in the σ-i regime can be evaluated by using the following empirical correlation (Hayashi et al., 2021):

$$\chi = 1 + 0.62We^{0.376} \tag{19}$$

where We is the Weber number defined by

$$We = \frac{\rho_L V_R^2 d}{\sigma} \tag{20}$$

It should be noted that, strictly speaking, this shape correlation obtained by fitting to the air-water data of $M = 2.63 \times 10^{-11}$ is applicable only to bubbles of the specific M. The use of this correlation for two-phase systems less viscous than the air-water system, however, may be justified as follows: Legendre et al. (2012) collected bubble shape data and conducted experiments to supplement the database. Based on the experimental data of χ they extended Moore's shape correlation by taking into account the viscous effect, i.e.

$$\chi = \left[1 - \frac{9}{64}\frac{We}{1 + K(M)We}\right]^{-1} \tag{21}$$

where the factor, $K(M)$, accounts for the effects of fluid property:

$$K(M) = 0.2M^{0.1} \tag{22}$$

Its value is small in the air-water system ($M \approx 10^{-11}$) and is also negligible in saturated steam-water system ($M \approx 10^{-13}$) as can be seen in Fig. 3. Therefore at M smaller than 10^{-11}, the correlation can be simplified to the original Moore correlation for small deformation:

$$\chi = 1 + \frac{9}{64} We \tag{23}$$

which is given in terms of We only. The empirical correlation, Eq. (19), for the σ-i regime obtained for the air-water system is thus expected to be applicable to lower Morton number systems.

Figure 4 shows C_L curves drawn by using the lift, drag and shape correlations described above. The lift curves agree well with the experimental data (Aoyama et al., 2017; Hessenkemper et al., 2021). It can be seen that the critical bubble Reynolds number increases with decreasing M. The lift reversal takes place in the μ regime and the σ-i regime, respectively, in Aoyama's data and Hessenkemper's data. Detailed discussion on Re_C will be given in Sec. 3.3.

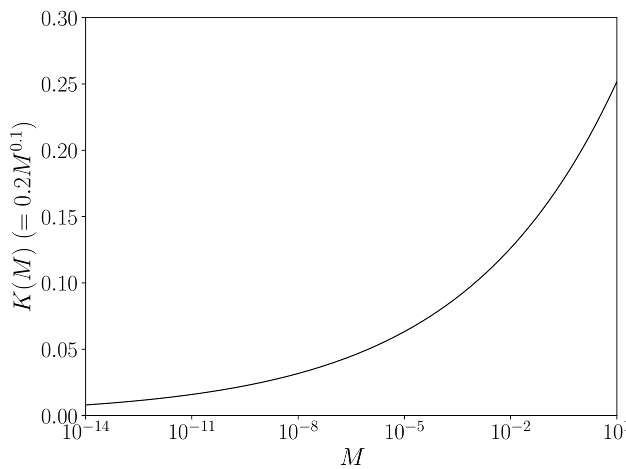

FIG. 3: Factor $K(M)$ in Legendre's shape correlation.

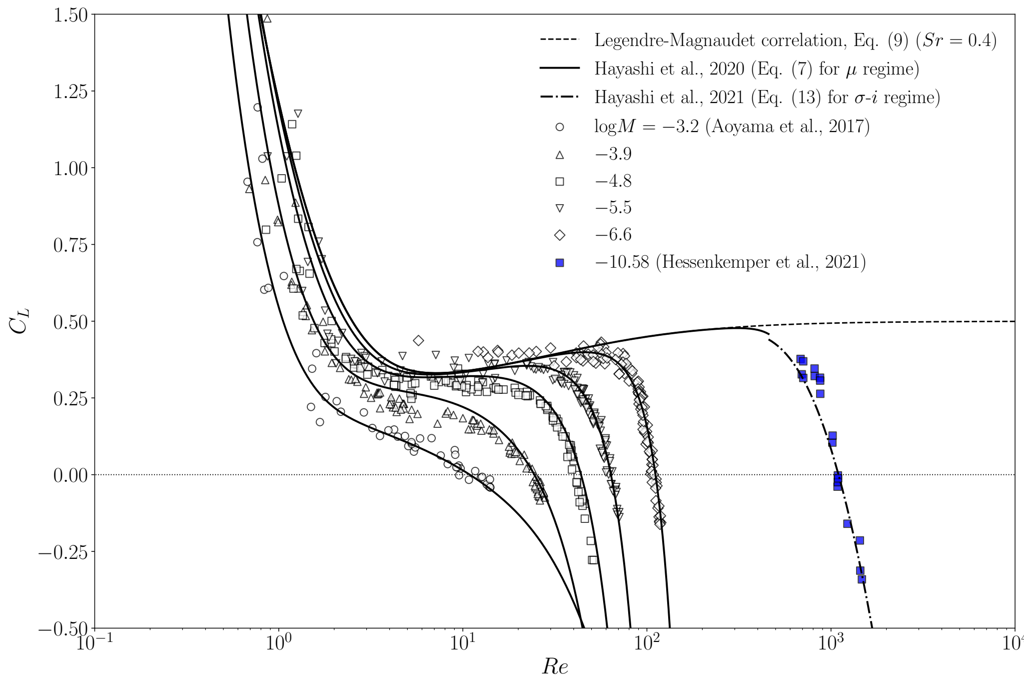

FIG. 4: Lift data (Aoyama et al., 2017; Hessenkemper et al., 2021) and lift curve drawn using empirical correlations. The lines are drawn with $Sr = 0.05$, 0.1, 0.2, 0.3, 0.4 and 0.4 for log$M = -3.2$, -3.9, -4.8, -5.5, -6.6 and -10.58, respectively.

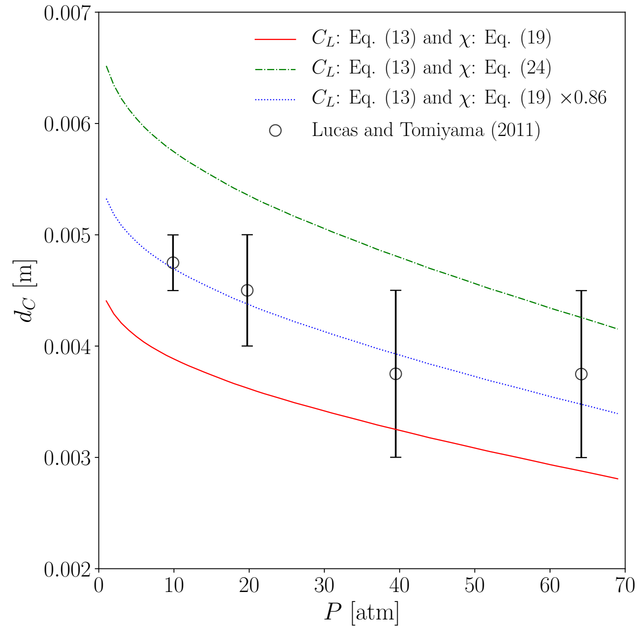

FIG. 5: Critical diameters in steam-water systems evaluated using C_L correlation.

3. CRITICAL BUBBLE DIAMETER

3.1 d_C in saturated steam-water systems

Figure 5 shows d_C calculated using the C_L correlation, Eq. (13), in comparison with the d_C data of the saturated steam-water systems (the pressure P ranging from 10 to 65 atm; void fraction less than 1%) (Lucas and Tomiyama, 2011), where the fitting equation $\chi(We)$, Eq. (19), for Hessenlemper's data of purified water was used for bubble shape. The correlation gives a reasonable trend of d_C, i.e. d_C are several millimeters and decrease with increasing the system pressure. However the d_C curve lies slightly below the data, implying that the χ correlation gives larger deformation. The dash-dotted line is drawn using the C_L correlation with the shape correlation proposed by Wellek et al. (1966):

$$\chi = 1 + 0.163 Eo^{0.757} \tag{24}$$

This equation is known to agree with χ of fully-contaminated bubbles (Tomiyama et al., 2002a). The d_C curve obtained with this shape correlation overestimates the data, and the data are within the two curves. The dotted line represents d_C calculated with Eq. (19), whereas the value of χ is reduced by 14% to make the prediction closer to the data. This curve agrees with the data. Colombet et al. (2015) reported that an effect of bubble swarm suppresses shape deformation. This effect explains a few percents of reduction in χ at void fractions of about 1%. The reasonable estimation of d_C allows us to use the C_L and χ correlations to evaluate d_C at M lower than that in the air-water system.

Figure 6 shows d_C plotted against M. The d_C is multivalued for M. Both μ_L and σ decrease with increasing P in the saturated steam-water system. The former steeply decreases at small P, whereas the decreasing rate becomes very small at about $P = 20$ atm. This is the cause of the non-monotonous dependence of M on P, i.e. M deceases with increasing P up to about 20 atm, and then it increases. During this change in M, d_C monotonously decreases.

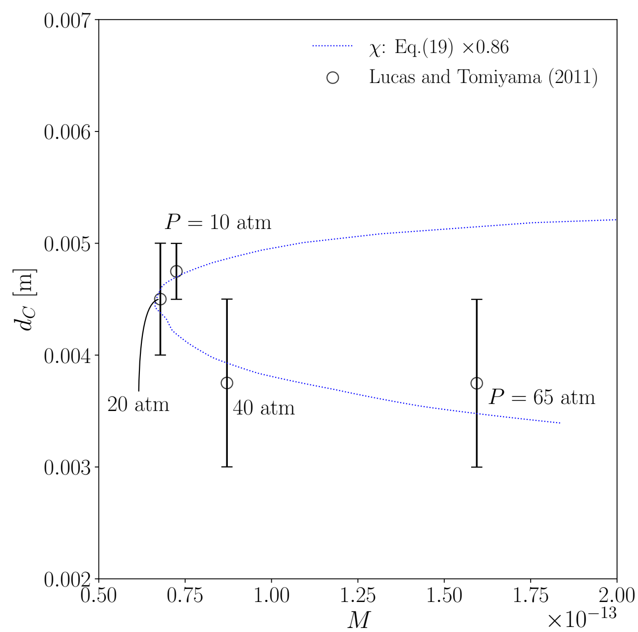

FIG. 6: Critical diameters in steam-water systems plotted against M.

3.2 d_C in air-water and air-glycerol water solution systems

Let us check the temperature dependence of d_C in the air-water system at atmospheric pressure. The broken line in Fig. 7 shows a d_C curve obtained by varying the temperature, T, from 273 to 373 K. Equation (13) for the σ-i regime was used. The d_C decreases from 4.9 mm at $T = 273$ K to 4.4 mm at $T = 373$ K with increasing T. Even with the significant change in T, d_C lies within the narrow band of ± 0.25 mm.

The data of air-glycerol water solutions were quoted from Aoyama et al. (2017). It should be noted that the lift reversal takes place in the μ regime in their experimental range (see Fig. 4). Therefore the lift curve was drawn by using Eq. (7) for the μ regime. With decreasing M, in other words with deceasing the glycerol concentration from 83 to 62 wt%, d_C somewhat increases and then decreases. The predicted d_C agrees well with the data. If we further decrease the glycerol concentration from 62 wt% ($\log M = -6.6$) down to 0% ($\log M = -11$), i.e. clean water, the d_C curve should reach the broken line of the air-water system. To meet this condition, the d_C curve of the air-glycerol water solution must change its trend so as to increase with decreasing M. This change would be caused by the transition from the μ regime to the σ-i regime.

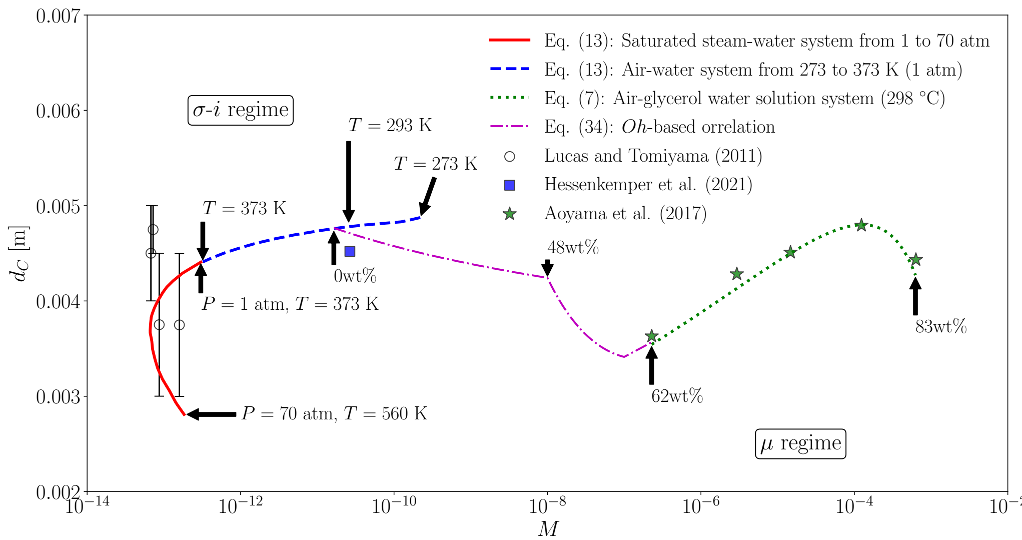

FIG. 7: Critical diameters in steam-water systems, air-water systems and air-glycerol water solution systems. The dash-dotted line is drawn using Eq. (34) to fill the gap between d_C of the glycerol-water solutions of 0 and 62 wt%.

3.3 Lift reversal criteria in terms of dimensionless groups

Figure 8 re-plots Re_C already shown in Fig. 2, whereas the Re_C curves here are drawn with the C_L correlations. Note that though the C_L correlations for the μ regime and the σ-i regime were validated for $-6.6 \leq \log M \leq -3.2$ and $\log M = -10.58$, respectively, they were also used for the gap, $-10.58 < \log M < -6.6$, to discuss the behavior of Re_C. The Re_C curve obtained by using Eq. (7) for the μ regime agrees well with Eq. (4) and seems to approach Re_O with decreasing M. On the other hand, the curve drawn by Eq. (13) for the σ-i regime shows good agreements with the data of the low viscosity systems. Hence by switching the Re_C curve depending on the regime the C_L-correlation-based Re_C criterion can cover the whole M range. The transition may take place between $\log M = -8$ and -7.

Figure 9 shows the critical Eo calculated using the C_L correlations. The shaded region represents a transition region estimated based on the characteristics of Re_C discussed above. In the σ-i regime the lift reversal criterion can be simply expressed as $Eo_C \approx 3$. This expression is much simpler than that in terms of Re_C shown in Fig. 8. In addition, d_C can be immediately calculated from Eo_C, provided that the fluid properties are given. The bubble terminal velocity, V_T, in infinite stagnant liquid for Eq. (18) is given by (Mendelson, 1967; Tomiyama et al., 1998)

$$V_T = \sqrt{\frac{\Delta\rho g d}{2\rho_L} + \frac{2\sigma}{\rho_L d}} \tag{25}$$

With this correlation, V_T decreases with increasing d due to the capillary effect up to a certain bubble diameter d_0, whereas it increases with d for $d > d_0$ as the inertia becomes dominant as shown in Fig. 10. The d_0 gives $Eo = 4$ and $d_0 \approx 5.4$ mm in the air-water system. The data of V_R in linear shear flows of contaminated water (Lee and Lee, 2020) are also plotted. The lift reversal takes place at $d = 6.1$ mm in their case. The data points of $C_L = 0$ lie around d_0 although Lee's

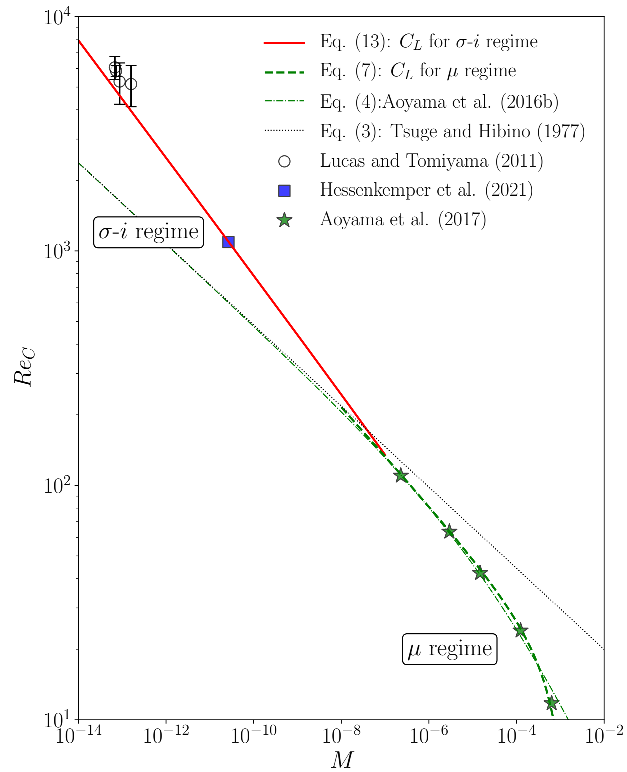

FIG. 8: Critical bubble Reynolds number, Re_C, calculated with C_L correlations.

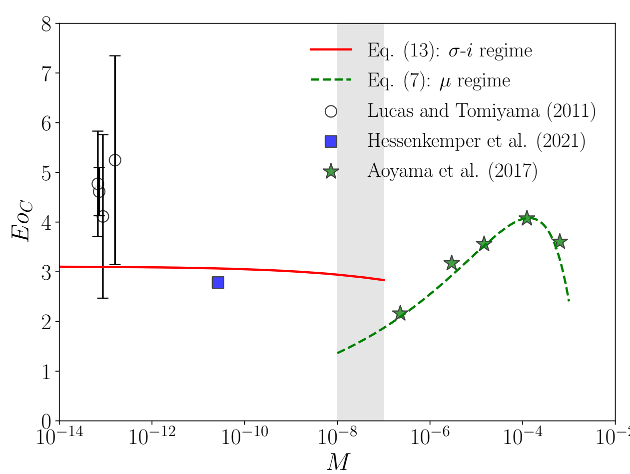

FIG. 9: Critical Eötvös number, Eo_C. The shaded region represents a transition region estimated based on the characteristics of Re_C.

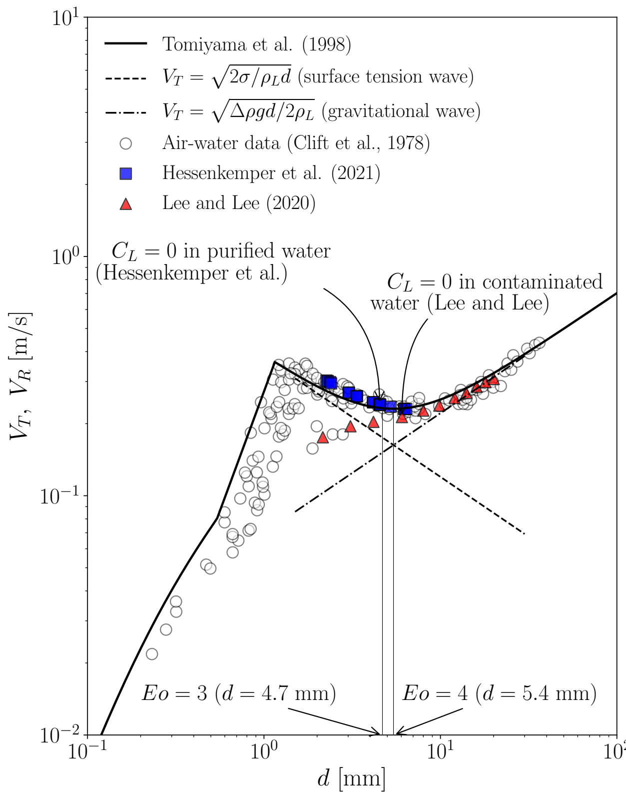

FIG. 10: Relative and terminal velocities of air bubbles in water.

data are for contaminated bubbles. Thus, it can be speculated that the lift reversal in the σ-i regime takes place around the bubble diameter for the transition of the dominant force between the surface tension force and inertia though more experimental data are required to validate this speculation.

In the μ regime, Eo_C shows a complex behavior as in the case with d_C. The cause of this complex trend in the μ regime has not been clarified yet. An ellipsoidal bubble in a high viscosity liquid may be able to keep fore-aft symmetric shape, whereas at low liquid viscosities the bubble shape tends to lose the fore-aft symmetry, i.e. the bubble front is to be flatten while the bubble rear would be still convex. Since the lift is very sensitive to the bubble shape, the distortion in bubble shape depending on M could be one of the reasons of the complex trend in Eo_C. Since the drag coefficient in the σ-i regime is given by $C_D = 8Eo/3(Eo{+}4)$, the almost constant Eo_C in the σ-i regime also means that the drag coefficient C_{DC} for Eo_C is more or less constant.

Figure 11 shows the modified Eötvös number, Eo_{HC}, for d_C, where Eo_H is defined by

$$Eo_H = \frac{\Delta\rho g d_H^2}{\sigma} \quad \left(= Eo\chi^{2/3}\right) \tag{26}$$

Being similar to the case with Eo_C, Eo_{HC} is almost constant in the σ-i regime and the value $Eo_{HC} \approx 4.8$ is close to Hessenkemper's data, i.e. 4.7. In the range of $10^{-5} < M < 10^{-4}$, the critical values are also around 5 even in the μ regime. This could be why Eo_H has often been

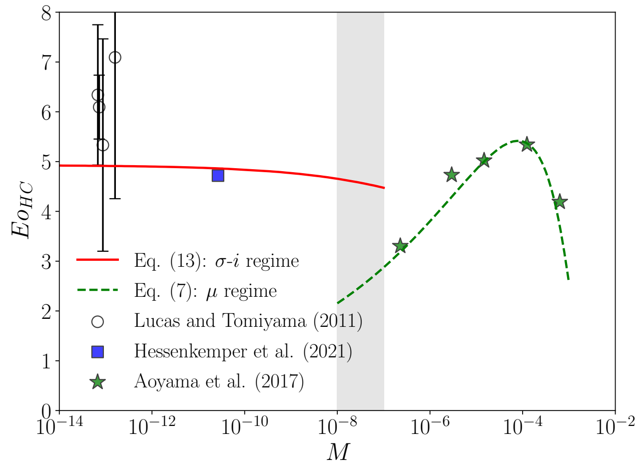

FIG. 11: Critical Eötvös number, Eo_{HC}, where Eo_H is the modified Eötvös number. Wellek's χ correlation and Aoyama's correlation were used to evaluate $Eo_{HC} = Eo_C\chi^{2/3}$ for the Lucas-Tomiyama data and for Aoyama's data, respectively.

used to correlate d_C in literature. However, the complex trend in the μ regime cannot be simply expressed in terms of Eo_H only as already pointed out in Aoyama et al. (2017) and Hayashi et al. (2020).

Since the bubble rise motion in the σ-i regime is governed by We rather than Re, We is expected to be another promising dimensionless group in the lift reversal criterion. Figure 12 shows the critical We. It should be noted that We is related with Eo and C_D as $We = 4Eo/3C_D$. The fact that We_C in the σ-i regime behaves in the same manner as Eo_C is not surprising; by applying the drag correlation, $C_D(Eo)$, We is expressed in terms of Eo:

$$We = \frac{1}{2}(Eo + 4) \tag{27}$$

The We_C in the μ regime is also approximately constant up to about $M = 10^{-5}$, whereas further increase in M decreases We_C.

The capillary number, Ca, defined by

$$Ca = \frac{\mu_L V_R}{\sigma} \tag{28}$$

is shown in Fig. 13. The Ca_C in the σ-i regime is very small due to the negligible effect of the viscous force on the bubble motion and can be fitted as (the cross symbols in the figure)

$$Ca_C = 1.434M^{0.2504} \tag{29}$$

If we take exactly $1/4$ for the power of M in this equation, we obtain the following relative velocity for the lift reversal in the σ-i regime:

$$V_R = 1.43\left[\frac{\Delta\rho g\sigma}{\rho_L^2}\right]^{1/4} \tag{30}$$

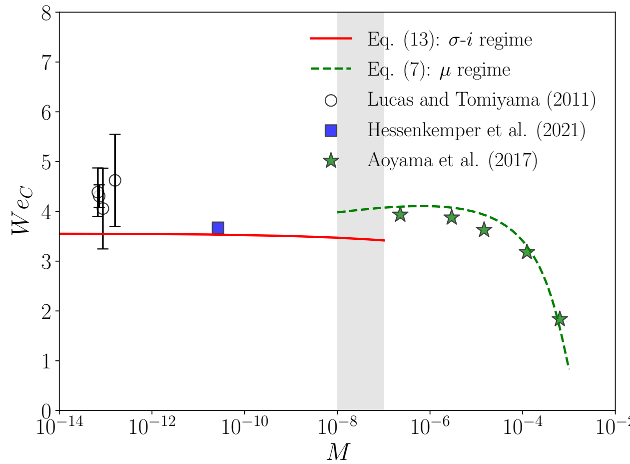

FIG. 12: Critical Weber number, We_C.

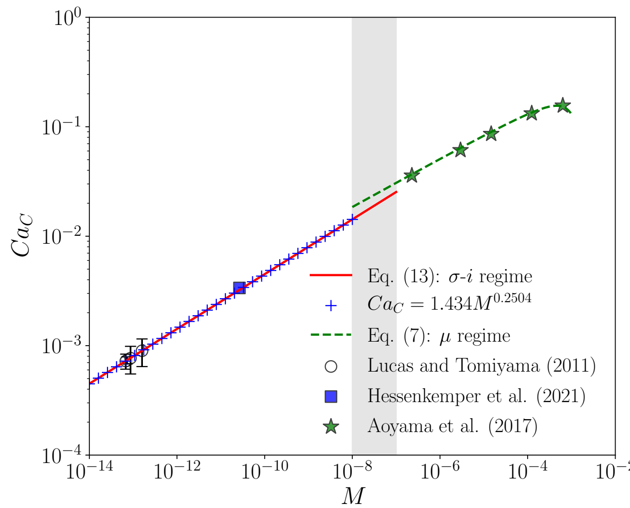

FIG. 13: Critical capillary number, Ca_C.

which is very similar to the minimum velocity given by Eq. (25) for d_0:

$$V_T = \sqrt{2}\left[\frac{\Delta\rho g\sigma}{\rho_L^2}\right]^{1/4} \tag{31}$$

Hence the speculation for the relation between the lift reversal and the transition of the dominant force made for the air-water system can be extended for other Morton number systems. Being similar to Eo_C, Ca_C exhibits a non-monotonic trend in the μ regime, i.e. Ca_C increases with increasing M up to $M \approx 5 \times 10^{-4}$ whereas decreases with further increase in M.

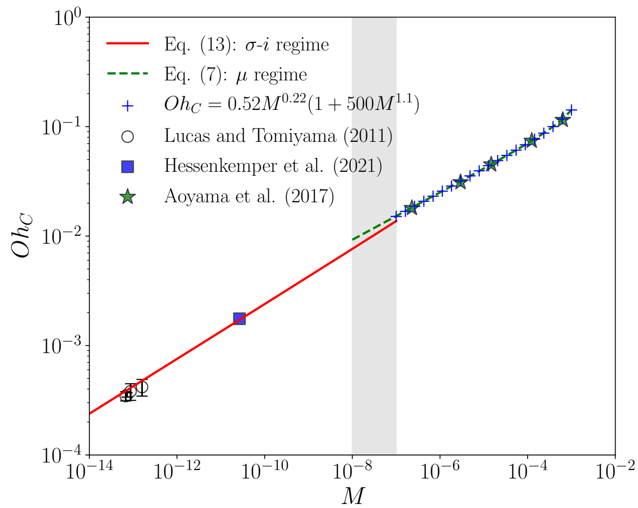

FIG. 14: Critical Ohnesorge number, Oh_C.

Figure 14 shows the Ohnesorge number, Oh, defined by

$$Oh = \frac{\mu_L}{\sqrt{\rho_L \sigma d}} \tag{32}$$

The Oh_C looks better to deal with the lift reversal criterion in the μ regime than Ca_C. The Oh can be expressed in terms of Ca and Re, i.e. $Oh = \sqrt{Ca/Re}$ or $Oh = \sqrt{We/Re^2}$, and therefore, three relevant forces, i.e. the inertial, the viscous and the surface tension forces are taken into account in Oh. Therefore the three forces should be taken into account in the lift reversal criterion to have a monotonous dependence on M in this regime. A fitting equation of Oh_C in terms of M can be obtained as

$$Oh_C = 0.52M^{0.22}\left(1 + 500M^{1.1}\right) \tag{33}$$

This equation is shown in Fig. 14 by the cross symbols.

Though the knowledge on d_C in the transition ($10^{-8} < M < 10^{-7}$) is still lacking, the following tentative correlation would be of use to evaluate d_C for a wide range of M:

$$Oh_C = \begin{cases} Oh_C^{\mu} & \text{for } M \geq 10^{-7} \\ Oh_C^{\sigma i} & \text{for } M \leq 10^{-8} \\ (\log M + 8)\left(Oh_C^{\mu} - Oh_C^{\sigma i}\right) + Oh_C^{\sigma i} & \text{for } 10^{-8} < M < 10^{-7} \end{cases} \tag{34}$$

where Oh_C^{μ} is given by Eq. (33) and $Oh_C^{\sigma i}$ is the Ohnesorge number evaluated with d_C for Eq. (29). Solving Eq. (25) for d_C with V_R given by Eq. (29) yields

$$\frac{d_C}{\sqrt{\sigma/\Delta\rho g}} = M^{-1/2}\left(Ca_C^2 \pm \sqrt{Ca_C^4 - 4M}\right) \tag{35}$$

We take the negative sign in the parentheses since $Eo_C < 4$ in the above analysis. The Oh_C in the transition regime is simply given as a linear interpolation of Oh_C^{μ} and $Oh_C^{\sigma i}$. The d_C of bubbles in glycerol-water solutions are evaluated with the correlation to fill the gap between 62wt% solution and clean water in Fig. 7, which confirms that the Oh-based correlation gives acceptable behavior of d_C depending on M. The correlation does not explicitly include V_R, and therefore, only the fluid properties are required for the evaluation of d_C.

4. CONCLUSION

The critical bubble diameter for the lift reversal was discussed in this study by making use of the available correlations of the lift coefficient, C_L, for clean bubbles in linear shear flows. The C_L correlations well describe the complex characteristics of the critical bubble diameter, d_C, for the lift reversal and the lift reversal criterion in terms of Re_C is reproduced well with the correlations. In the surface tension and inertial force dominant regime, i.e. the σ-i regime, the critical Eötvös and Weber numbers, Eo_C and We_C, can be used to develop a simple criterion of lift reversal, i.e. they are almost constant, and the critical capillary number, Ca_C, can be expressed in terms of the Morton number, M, only. These dimensionless groups in the viscous force dominant regime, i.e. the μ-regime, however show more complex dependences on M. On the other hand, the critical Ohnesorge number, Oh_C, monotonically increases with increasing M even in the viscous force dominant regime and can be fitted by a simple function in terms of M. The tentative correlation based on Oh is of use to evaluate d_C for a wide range of M.

ACKNOWLEDGMENTS

K. Hayashi and A. Tomiyama would like to express their thanks to financial supports by JSPS KAKENHI, Grant No. 20K04267 and 18H03756.

REFERENCES

Adoua, R., Legendre, D., and Magnaudet, J., Reversal of the lift force on an oblate bubble in a weakly viscous linear shear flow, *Journal of Fluid Mechanics*, vol. **628**, pp. 23–41, 2009.

Aoyama, S., Hayashi, K., Hosokawa, S., Lucas, D., and Tomiyama, A., Lift force acting on single bubbles in linear shear flows, *International Journal of Multiphase Flow*, vol. **96**, pp. 113–122, 2017.

Aoyama, S., Hayashi, K., Hosokawa, S., and Tomiyama, A., Shapes of ellipsoidal bubbles in infinite stagnant liquids, *International Journal of Multiphase Flow*, vol. **79**, pp. 23–30, 2016a.

Aoyama, S., Žun, Hayashi, K., Hosokawa, S., and Tomiyama, A., Lift force acting on single bubbles in linear shear flow, *the 9th International Conference for Multiphase Flow*, Firenze, Italy, 2016b.

Auton, T.R., The lift force on a spherical body in a rotational flow, *Journal of Fluid Mechanics*, vol. **183**, pp. 199–218, 1987.

Auton, T.R., Hunt, J.C.R., and Prud'homme, M., The force exerted on a body in inviscid unsteady non-uniform rotational flow, *Journal of Fluid Mechanics*, vol. **197**, pp. 241–257, 1988.

Bothe, D., Schmidtke, M., and Warnecke, H.J., VOF-simulation of the lift force for single bubbles in a simple shear flow, *Chemical Engineering Technology*, vol. **29**, pp. 1048–1053, 2006.

Chen, J., Hayashi, K., Hosokawa, S., and Tomiyama, A., Drag correlations of ellipsoidal bubbles in clean and fully-contaminated systems, *Multiphase Science and Technology*, vol. **31(3)**, pp. 215–234, 2019.

Colombet, D., Legendre, D., Risso, F., Cockx, A., and P., G., Dynamics and mass transfer of rising bubbles in a homogenous swarm at large gas volume fraction, *Jourla of Fluid Mechanics*, vol. **763**, pp. 254–285, 2015.

Dijkhuizen, W., van Sint Annaland, M., and Kuipers, J.A.M., Numerical and experimental investigation of lift force on single bubbles, *Chemical Engineering Science*, vol. **65**, pp. 1274–1287, 2010.

Ervin, E. and Tryggvason, G., The rise of bubbles in a vertical shear flow, *Journal of Fluids Engineering*, vol. **119**, pp. 443–448, 1997.

Hayashi, K., Hessenkemper, H., Lucas, D., Legendre, D., and Tomiyama, A., Scaling of lift reversal of deformed bubbles in air-water systems, *International Journal of Multiphase Flow*, p. 103653, 2021.

Hayashi, K., Legendre, D., and Tomiyama, A., Lift coefficients of clean ellipsoidal bubbles in linear shear flows, *International Journal of Multiphase Flow*, vol. **129**, p. 103350, 2020.

Hessenkemper, H., Ziegenhein, T., and Lucas, D., Contamination effects on the lift force of ellipsoidal air bubbles rising in saline water solutions, *Chemical Engineering Journal*, 2020.

Hessenkemper, H., Ziegenhein, T., Lucas, D., and Tomiyama, A., Lift force coefficient of ellipsoidal single bubbles in water, *International Journal of Multiphase Flow*, vol. **138**, p. 103587, 2021.

Lee, W. and Lee, J.Y., Experiment and modeling of lift force acting on single high Reynolds number bubbles rising in linear shear flow, *Experimental Thermal and Fluids Science*, vol. **115**, p. 110085, 2020.

Legendre, D., On the relation between the drag and the vorticity produced on a clean bubble, *Physics of Fluids*, vol. **19**, p. 018102, 2007.

Legendre, D. and Magnaudet, J., A note on the lift force on a spherical bubble or drop in a low-Reynolds-number shear flow, *Physics of Fluids*, vol. **9**, pp. 3572–3574, 1997.

Legendre, D. and Magnaudet, J., The lift force on a spherical bubble in a viscous linear shear flow, *Journal of Fluid Mechanics*, vol. **368**, pp. 81–126, 1998.

Legendre, D., Zenit, R., and Velez-Cordero, J.R., On the deformation of gas bubbles in liquids, *Physics of Fluids*, vol. **24(4)**, p. 043303, 2012.

Li, Z., Song, X., Jiang, S., and Ishii, M., The lateral migration of relative large bubble in simple shear flow in water, *Experimental Thermal and Fluid Science*, vol. **77**, pp. 144–158, 2016.

Lucas, D., Prasser, H.M., and Manera, A., Influence of the lift force on the stability of a bubble column, *Chemical Engineering Science*, vol. **60**, pp. 3609–3619, 2005.

Lucas, D. and Tomiyama, A., On the role of the lateral lift force in poly-dispersed bubbly flows, *International Journal of Multiphase Flow*, vol. **37**, pp. 1178–1190, 2011.

Magnaudet, J. and Mougin, G., Wake instability of a fixed spheroidal bubble, *Journal of Fluid Mechanics*, vol. **572**, pp. 311–337, 2007.

Mendelson, H.D., The prediction of bubble terminal velocities from wave theory, *AIChE Journal*, vol. **13(2)**, pp. 250–253, 1967.

Tomiyama, A., Struggle with computational bubble dynamics, *Multiphase Science and Technology*, vol. **10**, pp. 369–405, 1998.

Tomiyama, A., Celata, G., Hosokawa, S., and Yoshida, S., Terminal velocity of single bubbles in surface tension force dominant regime, *International Journal of Multiphase Flow*, vol. **28**, pp. 1497–1519, 2002a.

Tomiyama, A., Kataoka, I., Zun, I., and Sakaguchi, T., Drag coefficients of single bubbles under normal and micro gravity conditions, *JSME International Journal Ser. B: Fluids and Thermal Engineering*, vol. **41(2)**, pp. 472–479, 1998.

Tomiyama, A., Tamai, H., un, I., and Hosokawa, S., Transverse migration of single bubbles in simple shear flows, *Chemical Engineering Science*, vol. **57**, pp. 1849–1858, 2002b.

Tsuge, H. and Hibino, S., The onset conditions of oscillatory motion of single gas bubbles rising in various liquids, *Journal of Chemical Engineering of Japan*, vol. **10**, pp. 66–68, 1977.

Žun, I., The transverse migration of bubbles influenced by walls in vertical bubbly flow, *International*

Journal of Multiphase Flow, vol. **6**, pp. 583–588, 1980.

Wellek, R.M., Agrawal, A.K., and Skelland, A.H.P., Shapes of liquid drops moving in liquid media, *A.I.Ch.E. Journal*, vol. **12**, pp. 854–862, 1966.

Ziegenhein, T., Tomiyama, A., and Lucas, D., A new measuring concept to determine the lift force for distorted bubbles in low Morton number system: Results for air/water, *International Journal of Multiphase Flow*, vol. **108**, pp. 11–24, 2018.